Sea Breezes Shallow and Deep on the California Coast

ROBERT M. BANTA

Environmental Technology Laboratory, NOAA/ERL, Boulder, Colorado

7 July 1994 and 18 April 1995

ABSTRACT

Analyses of Doppler lidar data reveal sea breezes occurring on two different depth and time scales at Monterey Bay, California, on a day with offshore gradient flow indicated before sunrise and after sunset. The lidar data used in this study consist of vertical cross sections and profiles of the westerly, onshore wind component u. In the morning after 0900 PST a shallow sea breeze formed, which reached a depth of 300 m by noon. Starting in early afternoon a deeper sea-breeze layer formed in the lowest kilometer, and by late afternoon the shallow sea breeze blended into the deeper sea breeze and was no longer evident. Maximum speeds of 6 m s^{-1} in the shallow sea breeze occurred at the surface, whereas those in the deep sea breeze (also 6 m s^{-1}) were about 300 m above the surface. It is hypothesized that the shallow sea breeze is a local phenomenon responding to a more local temperature contrast between the sea and the region between the ocean and the mountain ranges. The deeper sea breeze, on the other hand, is seen as a more regional circulation, driven by the larger-scale contrast between the atmosphere over the ocean and that over the hot interior valleys of California, or perhaps even a larger continental scale. The lidar observations also included the evening transition, which began as a very shallow land breeze observed only by surface observing stations. In the deep sea-breeze layer between 250 m and 1 km AGL, the flow returned to offshore gradient flow simultaneously through the entire layer 2–4 h after sunset. The sea breeze was thus seen as a daytime interruption of the basic gradient offshore flow.

1. Introduction

Sea breezes occurring on two different length and time scales have been studied on both the east and the west coasts of the United States. On the East Coast, Atlas (1960) found both a sea breeze and a "mesoscale" or larger-scale sea breeze along the southern coast of Massachusetts using Doppler radar data. The mesoscale sea breeze was deeper (600 m) and formed later in the day than the smaller-scale sea breeze, which only reached a depth of 300 m. On the West Coast, Fosberg and Schroeder (1966) identified both a sea breeze and a "monsoon" flow, which had a diurnal character on many days (Fosberg 1992, personal communication), along the California coast north of San Francisco. In the present study, which took place along the coast of California at Monterey Bay just south of where Fosberg and Schroeder obtained their observations, we also found two different sea-breeze layers occurring on the same day. A shallow sea breeze began between 0900 and 1000 Pacific standard time (PST) but remained less than 300 m deep. After 1200 PST the flow in the layer between 300 m and 1 km reversed and began to flow onshore. As this deeper sea breeze strengthened, it produced a shear layer between 800 m and 1 km. The lower-level shear layer that had existed atop the shallow sea breeze at 300 m disappeared as the deeper sea breeze absorbed the shallower sea breeze. The instrument that produced these observations was a scanning Doppler lidar system developed by the Environmental Technology Laboratory (ETL) of the National Oceanic and Atmospheric Administration's Environmental Research Laboratories.

Understanding the sea breeze along the west coast of the United States and in other coastal regions is important for a great many reasons, as described by Schroeder et al. (1967), Simpson (1994), and in the recent National Research Council report on coastal meteorology (National Research Council 1992). These impacts include effects on fire weather, air pollution, aviation and military operations, agriculture, recreation, urban development, shipping, and transportation. The sea breeze also influences coastal ocean currents, which affect coastal erosion and beach development, coastal marine ecosystems, and activities such as fishing and shellfishing.

We recently used analyses of Doppler lidar scan data taken at Monterey Bay to reveal the structure of the shallow (<300 m deep) sea-breeze layer as it formed in midmorning and grew during afternoon hours (Banta et al. 1993, referred to hereafter as B93). In addition to showing consistency among lidar data, conventional data, and behavior expected from the sea breeze near the surface, the study highlighted many strengths of the

Corresponding author address: Dr. Robert M. Banta, U.S. Department of Commerce, NOAA/OAR/ERL/ETL, R/E/ET2, 325 Broadway, Boulder, CO 80303-3328.
E-mail: rbanta@etl.noaa.gov

Doppler lidar in studying small mesoscale phenomena. These included the lidar's ability to observe the presence or absence of flow layers by employing vertical-slice scans of Doppler velocity, and its ability to view horizontal variability of flows using scans in azimuth at low elevation angles.

The present study extends the analysis of the 16 September 1987 case in B93 and shows the development of a deep sea-breeze layer during midafternoon. As the deep sea breeze absorbed the earlier shallow sea-breeze layer, it produced an elevated wind speed maximum and was accompanied by a deceleration of flow at the surface. The deeper afternoon sea breeze is interpreted as a flow response to a larger, more regional scale of daytime surface temperature contrast between the cold waters offshore and the hot surface temperatures of the interior valleys of California. The shallow sea breeze, on the other hand, is interpreted as a response to a more local scale of forcing, most likely between the cold ocean and the low land between the shore and the first significant range of mountains.

2. The Land/Sea Breeze Experiment

Instrumentation was deployed to the Monterey Bay vicinity in September 1987 as a part of the Land/Sea Breeze Experiment (LASBEX). The instrumentation, which included surface meteorological stations, radiosonde, and Doppler sodars in addition to ETL's Doppler lidar, is described by Intrieri et al. (1990), Fagan (1988), Yetter (1990), and Shaw and Lind (1989). On 16 September a research vessel, the *Silver Prince,* was stationed 11 km offshore due west of the lidar. Onboard was an automated mesonet station for surface observations, and its crew performed three rawinsonde ascents on the present case study day.

The topography of the region (Fig. 1) consists of a complex shoreline, a coastal region with several parallel mountain ranges oriented north-northwest to south-southeast, and the interior valleys of California to the east of the extensive Diablo Range. These valleys are generally isolated by the mountains from the cooling effects of marine air, and thus they often attain very hot daytime surface temperatures (>40°C) in summer and early fall (B93; Intrieri et al. 1990).

Local times used in this paper are Pacific standard time, even though California was on daylight savings time during the experiment. The LASBEX study area is less than 2° longitude west of the central meridian for the Pacific time zone (120°W), and the 16 September date of the case in this study was within days of the autumnal equinox. Thus, sunrise and sunset were very nearly at 0600 and 1800 PST.

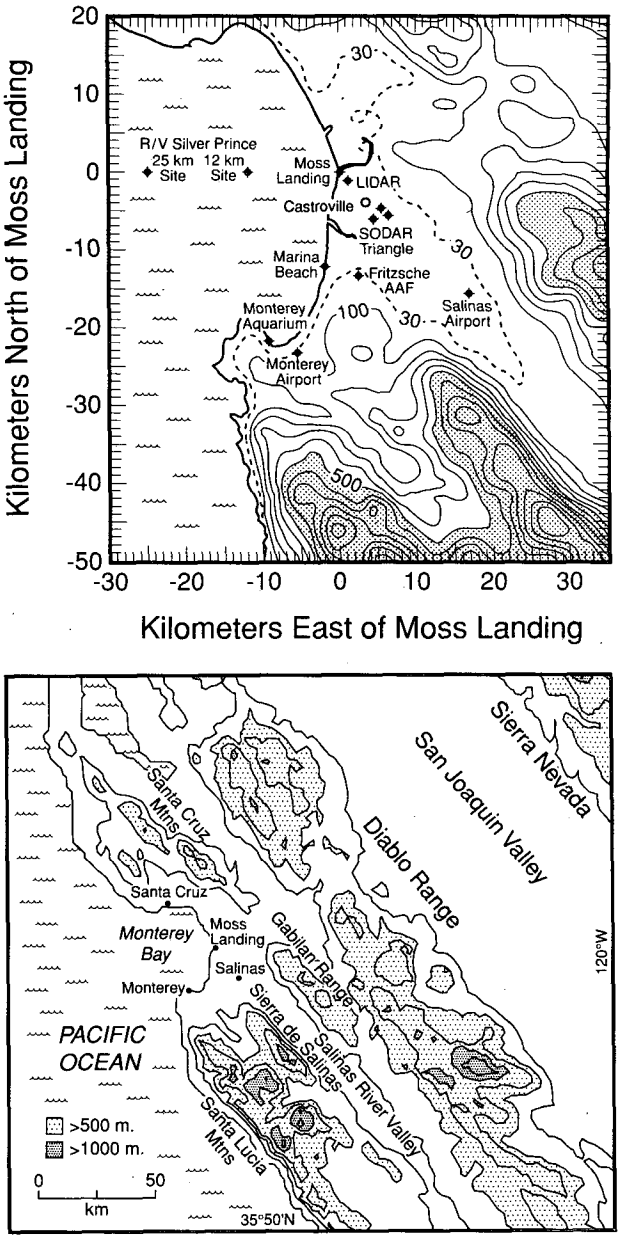

FIG. 1. Maps of the LASBEX experiment site. (a) Locations of sensors and sites with routine surface meteorological measurements in the local Monterey Bay area. The dashed terrain contour is 30 m above sea level. Solid terrain contours are at 100-m intervals. Terrain above 500 m is shaded (adapted from Fagan 1988). Castroville is located just northwest of the northern vertex of the sodar triangle. (b) Larger-scale map of the region. Mountain ranges and valleys affecting the coastal wind flows are shown. Terrain above 500 m has light shading and terrain greater than 1000 m has dark shading.

a. *Doppler lidar*

ETL's Doppler lidar is a scanning, active remote sensing instrument that transmits a coherent beam of 10.59-μm infrared (IR) light. A fraction of the transmitted light is scattered by aerosol particles and returns to the lidar. The signal is processed for backscattered intensity and frequency. The returned frequency provides a Doppler shift from which the radial velocity of

TABLE 1. Lidar parameters for LASBEX.

wavelength (μm)	10.59
maximum range (km)	up to 30
minimum range (km)	1.2
range resolution (m)	300
beamwidth (μrad) [°]	90 [0.005]
rms velocity accuracy (cm s^{-1})	60
pulse repetition frequency (Hz)	10
pulses averaged	3

the aerosols along the beam is calculated. The Doppler velocities indicated by the lidar represent the component of the wind along the lidar beam. Further details on the lidar as used during LASBEX are given in Table 1 and B93, and technical characteristics of the lidar are given by Post and Cupp (1990). Information on the usefulness of the lidar for studying other atmospheric phenomena is given by Banta et al. (1992) for a prescribed forest fire and Banta et al. (1995) for flows exiting a canyon in complex terrain.

b. *Synoptic conditions*

The larger-scale atmospheric conditions occurring on the case-study days in this paper have been described by B93. Normally, flow along the California coast during the warm season below about 1 km is onshore, because of the subtropical high pressure and cold ocean surface offshore (Johnson and O'Brien 1973), and the hot land surface and thermal low pressure inland (Fig. 2a). This onshore flow is very persistent during summer months (Wilczak et al. 1992; see their Fig. 2) and produces moderate (cool) temperatures inland (Fosberg and Schroeder 1966). On the other hand, on several occasions during the September days of LASBEX, including the present case study, cold fronts pushed south past Monterey Bay (Fig. 2b), leaving a layer of relatively cool air next to the surface. This "cold-air" layer was marked by a cold-advection shear region in the wind profile below 3 km AGL and offshore northeasterly flow in the lowest 0.5–1.5 km. The sea-breeze layers in the present study grew into this offshore gradient flow (B93). Ironically these kinds of post-cold-frontal days were dubbed "hot" days by Fosberg and Schroeder (1966), because the offshore flow inhibits the inland penetration of cool marine air and allows daytime temperatures inland to rise sharply from strong solar heating.

3. Results

Between 0900 and 1000 PST on the morning of 16 September a shallow sea-breeze layer developed and grew into the northeasterly offshore gradient flow as described by B93. In this section the afternoon transition to the deeper sea breeze and the evening transition back to gradient offshore flow below 2 km are described.

a. *Afternoon transition*

Vertical cross sections of u (Fig. 3) indicate a fundamental change in the structure of the afternoon onshore flow as the flow evolved from a shallow morning sea breeze into a deeper afternoon sea breeze. Figures 3a and 3c, reproduced from B93, show conditions be-

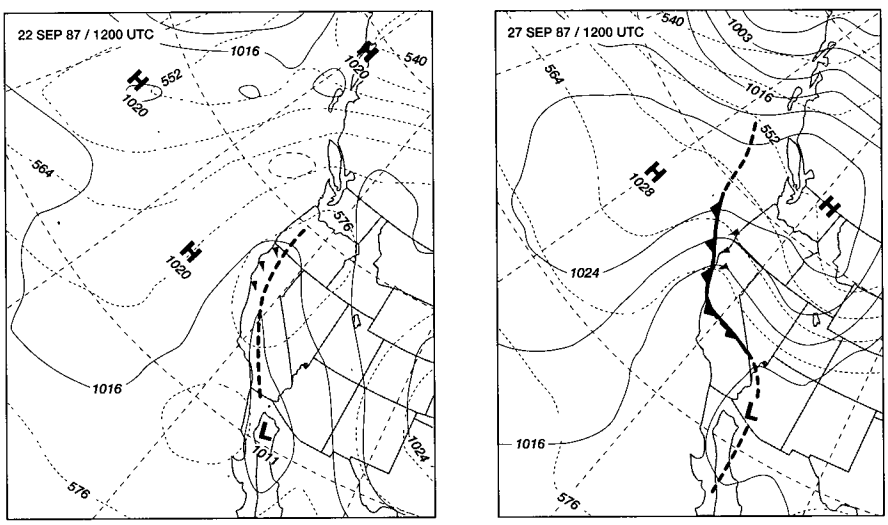

FIG. 2. Synoptic surface charts for (a) 0400 PST 22 September 1987, a day with onshore ambient flow at Monterey Bay, and (b) 27 September 1987, a day with offshore ambient flow. The pattern in (b) is almost identical to that on 16 September, the case study day in this paper. Solid contours represent sea level pressure in hectopascals, and dotted contours, 1000–500-hPa thickness in meters.

FIG. 3. Vertical cross sections of the u component of the wind on 16 September 1987. The lidar was positioned at (0,0), 1.5 km east of the shore. Monterey Bay is to the left (west), land to the right (east). Dashed lines indicate easterly flow and solid lines indicate westerly flow. (a) Offshore flow of 1-km depth at 1226 PST with the shallow sea breeze well established at the surface. (b) Dual sea-breeze flow at 1343 PST. (c) Deep sea-breeze flow at 1526 PST. Analysis grid spacing was 100 m in the horizontal and 25 m in the vertical. Time (PST) of the plot is in the upper left-hand corner.

fore and after this change, and Fig. 3b, the new cross section in this sequence, shows the interesting structure that occurred during the transition. Since the sea breeze was westerly, the lidar pointed directly up- or downwind with respect to the sea-breeze flow.

At 1226 PST (Fig. 3a), the maximum of greater than 6 m s^{-1} occurred at the surface, and the low-level flow was more turbulent over land. In the layer between 250 and 750 m the flow was nearly calm. This was a departure from earlier cross sections at 1217 PST and before, and in the *Silver Prince* rawinsonde wind profile at 1157 PST (Fig. 4). All showed easterly (offshore, $u < 0$) gradient flow in this layer, diminishing in time until the easterly flow at 1217 was very weak. The major shear zone was at the bottom of this layer, below about 300 m.

During the transition at 1343 PST (Fig. 3b) conditions below 250 m were similar to those at 1226 PST, in that the maximum speeds were still at the surface and turbulence was stronger over land. In the layer between 250 and 750 m, however, westerly, sea-breeze flow ($u > 0$) had accelerated to greater than 2 m s^{-1}. Figure 3b shows two major shear zones in the vertical, especially evident over the ocean. Between 800 and 600 m, u increased from -1 to 2 m s^{-1} moving downward through the layer, and again between 300 m and the surface the flow increased from 4 to 6 m s^{-1}. These shear zones were less evident over land, where vertical mixing induced by surface heating was more efficient. Thus, at this time, two sea-breeze layers were apparent, and this dual structure was reflected in the *Silver Prince* wind sounding at 1409 PST (reproduced in Fig. 4).

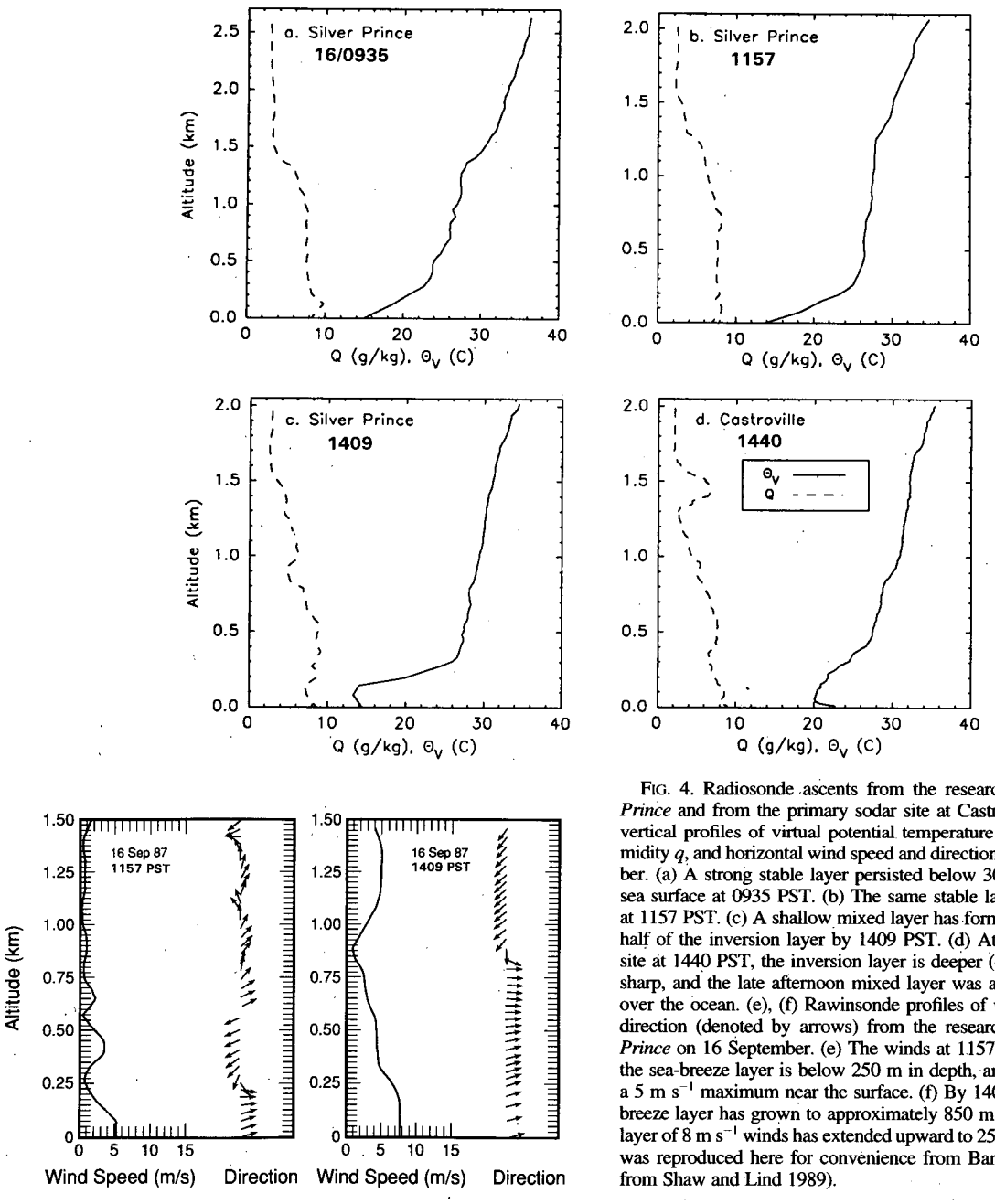

FIG. 4. Radiosonde ascents from the research vessel *Silver Prince* and from the primary sodar site at Castroville, showing vertical profiles of virtual potential temperature θ_v, specific humidity q, and horizontal wind speed and direction for 16 September. (a) A strong stable layer persisted below 300 m above the sea surface at 0935 PST. (b) The same stable layer is observed at 1157 PST. (c) A shallow mixed layer has formed in the lower half of the inversion layer by 1409 PST. (d) At the Castroville site at 1440 PST, the inversion layer is deeper (400 m) but less sharp, and the late afternoon mixed layer was also deeper than over the ocean. (e), (f) Rawinsonde profiles of wind speed and direction (denoted by arrows) from the research vessel *Silver Prince* on 16 September. (e) The winds at 1157 PST show that the sea-breeze layer is below 250 m in depth, and the wind has a 5 m s^{-1} maximum near the surface. (f) By 1409 PST the sea-breeze layer has grown to approximately 850 m in depth, and a layer of 8 m s^{-1} winds has extended upward to 250 m. This figure was reproduced here for convenience from Banta et al. (1993; from Shaw and Lind 1989).

The thermodynamic sounding also shows that the upper portion of the onshore flow layer, reaching approximately 500 m, extended up into the marine inversion layer.

Figure 3c (from B93) shows the culmination at 1526 PST of the radical change in structure. The entire layer between 100 and 750 m was moving onshore at about 6 m s^{-1}, and the only significant shear zone was at the top of the layer. The flow maximum in the vertical was no longer at the surface but was approximately 300 m above the surface. A simplistic explanation for this might be that surface friction retards the flow below 300 m. If the deep sea-breeze circulation resulted from the temperature contrast between California's interior valley and the ocean (as will be argued later in the conclusions), then the deep frictional influence would be due to the intervening mountain ranges acting as very tall roughness elements.

In addition to the 16 September findings, Banta et al. (1993) indicate (in their Table 3) that the dual sea-breeze structure shows up in early afternoon cross sections on all three of the other offshore-ambient-flow

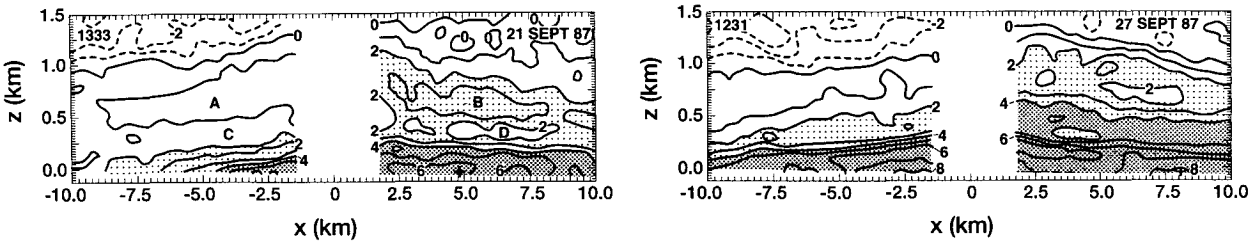

FIG. 5. Vertical lidar cross sections of the u component of the wind as in Fig. 3, showing the dual structure of the sea breeze. (a) 1333 PST 21 September cross section, showing where regions of higher-momentum flow (A,B) overlay regions of lower-momentum flow (C,D) in the developing upper sea-breeze layer. Cross indicates location of peak u value of 7 m s^{-1}. (b) The 1231 PST cross section on 27 September. Cross indicates maximum value of 8.4 m s^{-1}.

days during LASBEX when lidar data were available. Figure 5 gives examples of lidar cross sections from two of these days, showing the dual structure.

Vertical profiles of u constructed for 16 September from cross sections such as those in Fig. 3 give a somewhat more quantitative view of these changes. The profiles, shown for four times in Fig. 6, consist of values of u averaged over water from $x = -4$ to -1.5 km in Fig. 3. They indicate three overall strata. In the sea-breeze stratum (surface to 1 km) the profiles show the evolution from the shallow sea breeze to the deeper sea breeze, as discussed in the previous paragraph. The 1–2-km stratum could be interpreted as a return-flow layer for the deeper sea breeze, since offshore-flow speeds tended to increase as the afternoon proceeded. This interpretation is in contrast to the results of B93, who found that the *shallow* sea breeze had *no* return flow. The third stratum above 2 km responded to larger-scale flow. The negligible variations here indicate that this flow had little response to the diurnally forced changes below.

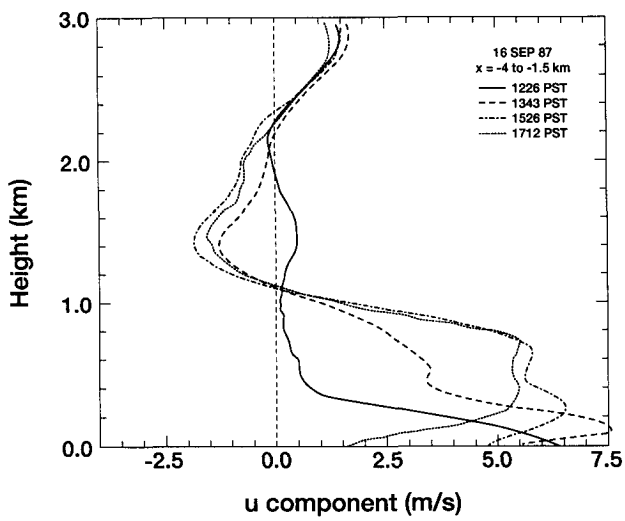

FIG. 6. Vertical profiles of the westerly wind u computed from vertical cross-section data as given in Fig. 3. Values at each level were averaged from $x = -4$ to -1.5 km.

The time–height cross section in Fig. 7 shows the values of u, averaged over the same horizontal region as the profiles in Fig. 6, contoured as a function of time and height. Data for the figure include 31 profiles between the surface and 3 km AGL spanning nearly 15 h, starting an hour after sunrise and ending approximately 4 h after sunset. This figure shows many of the features noted in Figs. 3–6, but with better time resolution. Before 1000 PST and below 1 km, strong negative u values indicate the period of postfrontal gradient flow off the land that had prevailed before sunrise. The shallow sea breeze began at the surface before 1000 and deepened gradually until 1200 PST, after which it grew rapidly. Aloft after about 0930 PST, the offshore flow in the layer between 250 and 750 m decelerated and reversed to onshore flow after 1200 PST; this deceleration is what led B93 to conclude that this was not a return flow compensating for the shallow sea breeze. The two-layer structure between 1300 and 1500 PST and the elevated wind speed maximum, which began at about 100 m AGL after 1330 PST and became an important characteristic of the fully developed deep sea breeze after 1500 PST, are also evident in the figure. The layer of offshore ($u < 0$) flow between 1 and 2 km from 1400 to 1900 PST again indicated characteristics of a return flow layer accompanying the deeper sea breeze. In addition to these features that were also noted in the discussion of Figs. 3–6, Fig. 7 shows the transition after sunset.

b. Evening transition

During the first hour after sunset at 1800 PST, little change occurred in the deep sea-breeze layer except at the surface. Data from mesonet stations (Fig. 8) showed that a land breeze was present at the surface beginning at approximately 1845 PST. The land breeze forms in a stable layer by surface cooling and is generally very shallow, especially early in the evening (Atkinson 1981). In this case the land-breeze layer was almost certainly only a few tens of meters deep and too shallow to be detected by the lidar. Over the next 2 h (from 1900 to 2100 PST), however, Fig. 7 shows that the entire layer *above* the surface decelerated. Although

FIG. 7. Time–height cross sections of the u component of the wind. Profiles were obtained by averaging grid points of cross-section data as in Fig. 3 from $x = -4$ to -1.5 km for each level from the surface to 4 km. Time is from left to right. Dashed lines represent flow from the east, solid lines flow from the west. Westerly flow 2–4 m s^{-1} has heavier shading, flow from 4 to 6 m s^{-1} has lighter shading, and flow less than 2 m s^{-1} or greater than 6 m s^{-1} has no shading. The maximum speed of 8 m s^{-1} occurred just after 1300 PST, 50–100 m above the surface. This figure extends Fig. 15 of Banta et al. (1993) in height to 2.5 km and in time of coverage to 2200 PST.

the changes were led by the lowest levels (below 250 m, 1800–1900 PST), the layer between 250 m and 1 km was especially noteworthy, because the change appears to have occurred simultaneously at all levels (i.e., the isotachs here are vertical and nearly parallel).

These processes are shown in more detail in the u profiles in Fig. 9. The deep sea breeze was well established in the 1712, 1808 (not shown), and 1844 PST profiles. After sunset the offshore-flow layer between 1 and 2 km AGL accelerated (1844, 1910 PST). Deceleration of the deep sea-breeze layer was evident in profiles at 1910, 1935 (not shown), and 2004 PST, and deceleration of the return flow layer, in the 1935 (not shown) and 2004 PST profiles. At the surface prior to 2004 PST the land breeze was too shallow to be detected by the lidar in these profiles as described above. Profiles after 2004 PST (Fig. 9b) show the progressive reestablishment of offshore gradient flow between the surface and 1.5 km AGL.

4. Conclusions

Because the topography of California is highly complex, it should perhaps not be surprising that the sea breeze along the California coast is also complex. On a day with ambient offshore gradient flow in the lowest 1–2 km, a shallow sea-breeze layer formed and grew to 300 m by noon. In the afternoon, starting just before 1300 PST, a deeper sea-breeze layer reversed the gradient offshore flow below 1 km AGL. This deeper onshore flow layer persisted until after sunset, when the flow below 1 km rapidly returned to the original offshore direction. The sea breezes can be viewed, therefore, as a daytime interruption below 1 km of the offshore gradient wind pattern that existed before sunrise and resumed after sunset. In other words, the mesoscale pressure gradient, provided by the differential heating mechanism that drove the deep sea breeze, was temporarily strong enough to overcome the synoptic postfrontal pressure gradient. But soon after the daytime forcing ceased, the synoptic pressure gradient again dominated, and the flow above the land breeze in the lowest kilometer shifted back to offshore.

How representative of the meteorology of this region was this case study day? The only offshore-ambient-flow day when the lidar operated into the late afternoon and evening was 16 September. On three other offshore-flow days during LASBEX, however, lidar data were taken through about midafternoon. On each of these days, both the incipient deep sea breeze and the dual structure as seen in Fig. 3 were noted in the early afternoon cross sections. Thus, it appears that the deep sea breeze is a recurrent phenomenon in this and perhaps other similar regions. Surface observations in several studies indicate that this may occur in other regions of the globe, including Massachusetts on the east coast

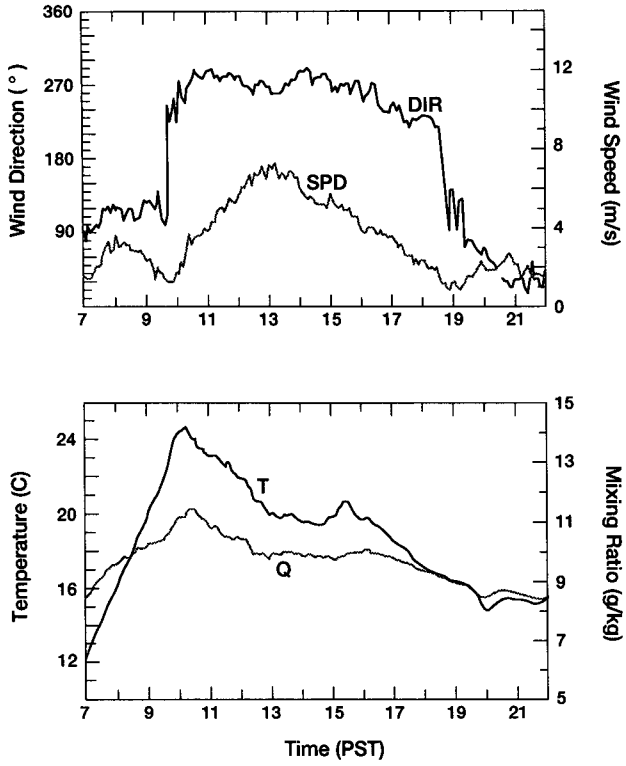

FIG. 8. Time series of (a) wind direction, speed, and (b) temperature and water vapor mixing ratio on a 27-m mast at the northernmost vertex of sodar triangle near Castroville (NEPRF station). Transition to westerly component flow (sea breeze) at 1015 PST and back to easterly component flow (land breeze) at 1845 PST can be seen. Observations were recorded at 20-s time intervals.

of the United States (Atlas 1960), Australia (Physick and Byron-Scott 1977, Simpson 1994), and Sweden (Borne 1994). In these studies the direction of the sea breeze at the surface in the morning is completely different from the direction later in the day. The morning sea breeze blows perpendicular to the local coastline, whereas the later flow is from the ocean to a larger-scale land mass.

A few characteristics of the shallow sea breeze in this region as described by B93 can be compared with characteristics of the deeper sea breeze in the present study. In the shallow sea breeze, the peak wind speeds are at the surface, whereas in the fully developed deeper sea breeze they were about 300 m above the surface. The shallow sea breeze shows no evidence of a return flow, but the deeper sea breeze did exhibit a flow aloft that had characteristics of a return-flow layer. It is hypothesized that the shallow sea breeze was driven by a more local temperature contrast between the sea and one of the mountain ranges to the east, whereas the deep sea breeze was a response to a larger scale of forcing: the atmosphere heated to a great depth (perhaps as much as 3 km AGL) over inland California, whereas over the sea, the atmosphere above 300 m was not heated by underlying surfaces.

In spite of the detail obtainable from the lidar observations, a number of questions remain. Why did the surface flow decelerate after the transition to the deeper, regional sea breeze? If the flow atop the regional sea breeze really was a return flow, why was no Coriolis turning of the flow observed (Atkinson 1981; Banta et al. 1993)? What was the scale and nature of the forcing for the regional (deep) sea breeze? The forcing could have been the contrast between the ocean and the interior valleys, or it could have been even a larger, more continental scale as suggested by Fosberg and Schroeder (1966). Was the nature of the solenoidal flow in this layer predominantly land–sea temperature

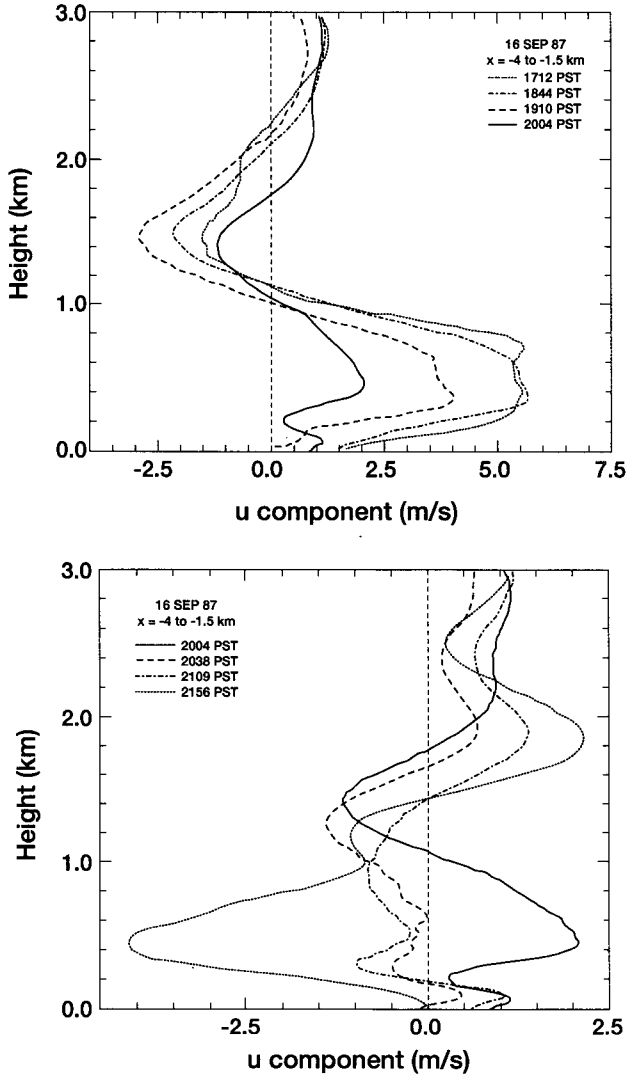

FIG. 9. Vertical profiles of u as in Fig. 5 for (a) 1712, 1844, 1910, and 2004 PST, and (b) 2004 (repeated), 2038, 2109, and 2156 PST. Values were averaged from $x = -4$ to -1.5 km for each level.

contrast, or could it have had an anabatic component from the larger-scale mountainous topography inland?

These and other important questions can be addressed by numerical modeling, since nested-grid techniques and massively parallel systems now allow more than one scale of forcing to be studied simultaneously. Of course, the issues can (and should) also be addressed observationally. For example, Doppler lidar deployed together with a network of UHF profilers equipped with radio acoustic sounding systems (RASS) to determine both wind and temperature profiles, and with conventional instrumentation, would allow the structure and extent of both large- and small-scale systems to be monitored and studied.

Acknowledgments. I thank Lisa Olivier, David Levinson, and Zhu Cui-Juan, who performed the laborious reduction and analysis of the lidar data used in this study, and I thank the members of the lidar group, including Richard Cupp, Freeman Hall, and the other "crew members," who obtained the data used in this study. I also appreciate the contributions of the following for their roles in organizing and operating LASBEX: Gordon Little, William Shaw, Tak Cheung, and our colleagues Janet Intrieri and William Shaw for helpful discussions of LASBEX and the Monterey Bay sea breeze. Janet Intrieri and Taneil Uttal provided helpful reviews of the manuscript.

REFERENCES

Atkinson, B. W., 1981: *Mesoscale Atmospheric Circulations.* Academic Press, 125–214.

Atlas, D., 1960: Radar detection of the sea breeze. *J. Meteor.,* **17,** 244–258.

Banta, R. M., L. D. Olivier, E. T. Holloway, R. A. Kropfli, B. W. Bartram, R. E. Cupp, and M. J. Post, 1992: Smoke column observations from two forest fires using Doppler lidar and Doppler radar. *J. Appl. Meteor.,* **31,** 1328–1349.

——, ——, and D. H. Levinson, 1993: Evolution of the Monterey Bay sea-breeze layer as observed by pulsed Doppler lidar. *J. Atmos. Sci.,* **50,** 3959–3982.

——, ——, W. D. Neff, D. H. Levinson, and D. Ruffieux, 1995: Influence of canyon induced flows on flow and dispersion over adjacent plains. *Theor. Appl. Climatol.,* **50,** in press.

Borne, K., 1994: Sea and land breeze at the Swedish west coast. Preprints, *Second Int. Conf. on Air–Sea Interaction and on Meteorology and Oceanography of the Coastal Zone.* Lisbon, Portugal, Amer. Meteor. Soc., 182–183.

Fagan, M., 1988: The sea breeze circulation during the Land Sea Breeze Experiment (LASBEX) in central California. M.S. thesis, Dept. of Meteorology, Naval Postgraduate School, 127 pp.

Fosberg, M. A., and M. J. Schroeder, 1966: Marine air penetration in central California. *J. Appl. Meteor.,* **5,** 573–589.

Intrieri, J. M., C. G. Little, W. J. Shaw, R. M. Banta, P. A. Durkee, and R. M. Hardesty, 1990: The Land/Sea Breeze Experiment (LASBEX). *Bull. Amer. Meteor. Soc.,* **71,** 656–664.

Johnson, A., Jr., and J. J. O'Brien, 1973: A study of an Oregon sea breeze event. *J. Appl. Meteor.,* **12,** 1267–1283.

National Research Council, 1992: *Coastal Meteorology: A Review of the State of the Science.* National Academy Press, 99 pp.

Physick, W. L., and R. A. D. Byron Scott, 1977: Observations of the sea breeze in the vicinity of a gulf. *Weather,* **32,** 373–381.

Post, M. J., and R. E. Cupp, 1990: Optimizing a pulsed Doppler lidar. *Appl. Opt.,* **29,** 4145–4158.

Schroeder, M. J., M. A. Fosberg, O. P. Cramer, and C. A. O'Dell, 1967: Marine air invasion of the Pacific coast: A problem analysis. *Bull. Amer. Meteor. Soc.,* **48,** 802–808.

Shaw, W. J., and R. J. Lind, 1989: Sounding and surface meteorological data from the Land/Sea Breeze Experiment (LASBEX). NPS-63-90-001, Naval Postgraduate School, 294 pp.

Simpson, J. E., 1994: *Sea Breeze and Local Winds.* Cambridge University Press, 234 pp.

Wilczak, J. M., M. L. Cancillo, and C. W. King, 1992: Observations of mesoscale flows in northern California using an array of wind profilers. *Proc. Sixth Conf. on Mountain Meteorology,* Portland, OR, Amer. Meteor. Soc., 222–227.

Yetter, J. A., 1990: The nature of the propagation of sea breeze fronts in central California. M.S. thesis, Dept. of Meteorology, Naval Postgraduate School, 65 pp.